DALTON
FULL PAPER

Revisiting the synthesis of $[Mo_6(\eta^5\text{-}C_5Me_5)O_{18}]^-$. X-Ray structural analysis, UV-visible, electrochemical and multinuclear NMR characterization

Anna Proust,* René Thouvenot and Patrick Herson

Laboratoire de Chimie Inorganique et Matériaux Moléculaires, ESA 7071, Université Pierre et Marie Curie, 4 Place Jussieu, Case 42, 75252 Paris Cedex 05, France. E-Mail: proust@ccr.jussieu.fr

Received 27th July 1998, Accepted 2nd November 1998

In methanol, $[n\text{-}Bu_4N][MoCp^*O_3]$ reacted with $[n\text{-}Bu_4N]_2[Mo_4O_{10}(OMe)_4Cl_2]$ to yield $[n\text{-}Bu_4N][Mo_6Cp^*O_{18}]$ in reasonable yield, thus opening a new route in the synthesis of organometallic derivatives of polyoxometalates. The crystal and molecular structure of $[n\text{-}Bu_4N][Mo_6Cp^*O_{18}]\cdot Me_2CO$ has been determined by single-crystal X-ray diffraction. The ion $[Mo_6Cp^*O_{18}]^-$ has been thoroughly characterized by multinuclear NMR in solution. The ^{95}Mo and ^{17}O NMR data support the conclusion that the Cp* ligand is a better $\sigma + \pi$ donor than the oxo ligand. The complex is electrochemically active and displays three successive one-electron reduction processes.

As it provides an understanding of oxide surface reactions at the molecular level, the chemistry of organometallic derivatives of soluble oxide analogues is rapidly expanding. A significant class of compounds comprises organometallic derivatives of polyoxometalates[1] with major contributions from Klemperer, Finke and Isobe's groups. Oligomerization of oxometalates in the presence of $[(RhCp^*Cl_2)_2]$ allowed Isobe[2] to obtain molecular cubane-type clusters, which mimic the structure as well as the reactivity of bulk oxides. In the case of $[(RhCp^*)_4V_6O_{19}]$ the Cp^*Rh^{2+} fragments stabilize the otherwise unstable $\{V_6O_{19}\}^{8-}$ core.[3,4] On the other hand, the polyanion-supported organometallic complexes described by Day and Klemperer[5] and Finke and co-workers[6–11] are rather relevant to the modeling of organometallic catalyst oxide–support interactions. Determination of their molecular and electronic structures either by single-crystal X-ray diffraction or by spectroscopic methods affords accurate structural and spectroscopic models for interfacial organometallic chemistry. The relative basicities of the oxo ligands, an essential factor in oxide surface reactivity, can also be assessed from studies of the fixation of organometallic units onto the polyoxometallic framework. Most interestingly, the Dawson-type $[P_2W_{15}Nb_3O_{62}]^{9-}$ polyoxoanion-supported $Re(CO)_3^+$ and $Ir(CO)_2^+$ complexes provide models for the mobility of $M(CO)_n^+$ cations on an oxide surface.[12] On the other hand, $[(1,5\text{-}COD)IrP_2W_{15}Nb_3O_{62}]^{8-}$ displays its own reactivity either as a catalyst[13] or as a precursor for polyoxoanion-stabilized $Ir_{\approx 300}$ nanoclusters.[14] Moreover, organometallic derivatives of polyoxoanions could also display synergistic effects or even bifunctional activity.[15]

In the course of their extensive investigation of cyclopentadienyl–oxo complexes,[16] Bottomley and co-workers described the crystal structure of $[C_5Me_5O][Mo_6Cp^*O_{18}]$, obtained by air oxidation of $[\{MoCp^*(CO)_2\}_2]$ in $CHCl_3$.[17] This prompted us to benefit from our experience in the functionalization of polyoxometalates[18–23] for developing a more straightforward synthesis for $[Mo_6Cp^*O_{18}]^-$ and similar complexes. This paper addresses an alternative preparation of $[Mo_6Cp^*O_{18}]^-$ by self-assembly of $[MoCp^*O_3]^-$ and oxomolybdenum fragments generated from the $[Mo_4O_{10}(OMe)_4Cl_2]^{2-}$ anion. The single-crystal structure analysis of $[n\text{-}Bu_4N][Mo_6Cp^*O_{18}]\cdot Me_2CO$ and the characterization of $[Mo_6Cp^*O_{18}]^-$ by multinuclear NMR (^1H, ^{13}C, ^{17}O and ^{95}Mo), UV-visible spectroscopy and electrochemistry are reported.

Experimental

Dimethylhydroxylamine hydrochloride, tetrabutylammonium hydroxide 1 M in methanol and HPLC grade acetonitrile were purchased from Aldrich and used as received. Reagent grade methanol was distilled over magnesium methoxide. The salt $[n\text{-}Bu_4N]_4[\alpha\text{-}Mo_8O_{26}]$ was synthesized according to the published procedure and recrystallized in acetonitrile,[24] $[n\text{-}Bu_4N][MoCp^*O_3]$ by addition of 1 equivalent of $n\text{-}Bu_4NOH$ to a solution of $[t\text{-}BuNH_3][MoCp^*O_3]$ in methylene chloride, prepared as described.[25] The salt $[n\text{-}Bu_4N][BF_4]$ was prepared from $[n\text{-}Bu_4N][HSO_4]$ and $NaBF_4$ and dried overnight at 80 °C under vacuum.

Infrared spectra were recorded from KBr pellets on a Bio-Rad FT 165 spectrophotometer, electronic absorption spectra on a Shimadzu model UV-2101 spectrophotometer. Elemental analyses were performed at Pierre et Marie Curie University or at the Service Central d'Analyse of the Centre National de la Recherche Scientifique (Vernaison, France). Proton and ^{13}C NMR spectra were recorded in 5 mm o.d. tubes at room temperature on a Bruker AC300 spectrometer, natural abundance ^{17}O and ^{95}Mo NMR spectra from CH_3CN–CD_3CN (2 cm^3–0.2 cm^3) solutions in conventional 10 mm o.d. tubes at 343 K on a Bruker AM500 spectrometer.

Preparation of $[n\text{-}Bu_4N]_2[Mo_4O_{10}(OMe)_4Cl_2]$

To a suspension of $[n\text{-}Bu_4N]_4[\alpha\text{-}Mo_8O_{26}]$ (2.15 g, 1 mmol) in methanol (15 cm^3) were added 1.91 g (20 mmol) of $Me_2NOH\cdot HCl$. The mixture was heated to reflux until a clear green solution was obtained, which was then allowed to cool slowly to room temperature. Within a few hours, colourless crystals of $[n\text{-}Bu_4N]_2[Mo_4O_{10}(OMe)_4Cl_2]$ deposited (1.35 g, 55%); $\tilde{\nu}_{max}$/cm^{-1} 2962s, 2932m, 2876m, 2822w, 1474m, 1382w, 1025m, 993m, 941s, 917vs, 900s, 738w, 705s, 598w, 548m, 380w, 344w and 311m (Found: C, 35.54; H, 7.02; N, 2.25. $C_{18}H_{42}ClMo_2NO_7$ requires C, 35.34; H, 6.92; N, 2.29%).

Preparation of $[n\text{-}Bu_4N][Mo_6Cp^*O_{18}]$

In a typical experiment, a solution of 0.39 g (0.75 mmol) of $[n\text{-}Bu_4N][MoCp^*O_3]$ in 25 cm^3 of methanol was added to a suspension of 0.979 g (0.8 mmol) of $[n\text{-}Bu_4N]_2[Mo_4O_{10}(OMe)_4Cl_2]$ in 25 cm^3 of methanol. After a 1.5 h reflux, the solution was

concentrated to about 40 cm^3 and set aside at room temperature. After a few days, 0.2 g of $[n\text{-}Bu_4N][Mo_6Cp^*O_{18}]$ was collected as orange-red crystals, which proved too small for an X-ray analysis. A further crop of compound was isolated from the filtrate later on (whole yield 40%, based on $[n\text{-}Bu_4N][MoCp^*O_3]$); $\tilde{\nu}_{max}/cm^{-1}$ 2963m, 2929m, 2874w, 1472w, 1442w, 1372w, 982m, 955s, 798s and 778s (Found: C, 25.66; H, 4.22; Mo, 44.32; N, 1.08. $C_{26}H_{51}Mo_6NO_{18}$ requires C, 25.16; H, 4.14; Mo, 46.37; N, 1.12%); λ_{max}/nm (log ε/$dm^3\ mol^{-1}\ cm^{-1}$) (CH_3CN) 258 (4.5), 283 (sh) (4.4) and 494 (sh) (2.35); δ_H(300.13 MHz; solvent acetone-d_6; standard $SiMe_4$) 2.23 [15 H, s, $C_5(CH_3)_5$], 3.33 [8 H, m, $N(CH_2CH_2CH_2CH_3)_4$], 1.65 [8 H, m, $N(CH_2CH_2CH_2CH_3)_4$], 1.43 [8 H, m, $N(CH_2CH_2CH_2CH_3)_4$] and 0.99 [12 H, t, $N(CH_2CH_2CH_2CH_3)_4$]; δ_C(75.47 MHz; solvent CD_3CN; standard $SiMe_4$) 140.0 [5 C, $C_5(CH_3)_5$] and 12.6 [5 C, $C_5(CH_3)_5$], 59.9 [4 C, $N(CH_2CH_2CH_2CH_3)_4$], 24.9 [4 C, $N(CH_2CH_2CH_2CH_3)_4$], 20.9 [4 C, $N(CH_2CH_2CH_2CH_3)_4$] and 14.4 [4 C, $N(CH_2CH_2CH_2CH_3)_4$]; $\delta_{95_{Mo}}$(32.6 MHz; solvent CH_3CN–CD_3CN, 343 K; standard aqueous alkaline Na_2MoO_4) 175 (1 Mo, Mo_{axial}), 164 (4 Mo, $Mo_{equatorial}$) and −35 (1 Mo, Cp*Mo); δ_{17O}(67.8 MHz; solvent CH_3CN–CD_3CN, 343 K; standard distilled water) 931 (4 O, $O_{terminal}$), 890 (1 O, $O_{terminal}$), 613 (4 O, μ-O), 580 (4 O, μ-O), 559 (4 O, μ-O) and −2.7 (1 O, μ_6-O). Suitable crystals for an X-ray diffraction study were grown from an acetone solution of the crude compound. Their IR spectrum was very similar to that of the crystals obtained in methanol except for two additional bands at 1708 and 1224 cm^{-1}, attributed to acetone molecules. Cell parameters have also been determined for crystals obtained from a solution of the compound in acetonitrile : tetragonal, $a = b = 18.349(8)$, $c = 51.02(3)$ Å, $U = 17179(23)$ $Å^3$.

Electrochemistry

All measurements were carried out in acetonitrile, under nitrogen, at room temperature, by using a standard three-electrode cell, which consisted of the working electrode, an auxiliary platinum electrode, and an aqueous saturated calomel electrode (SCE) equipped with a double junction. Solution concentrations were *ca*. 1 mM for the compound and 0.1 M for the supporting electrolyte, $[n\text{-}Bu_4N][BF_4]$. Polarograms were recorded at a dropping mercury electrode on a Tacussel PRG3 device, at the rate of 0.15 V min^{-1}. Cyclic voltammograms were recorded at a carbon electrode on a PAR 273 instrument, at the rate of 0.1 V s^{-1}.

Crystal structure determination for $[n\text{-}Bu_4N][Mo_6Cp^*O_{18}]\cdot Me_2CO$

Crystal data. $C_{29}H_{57}Mo_6NO_{19}$, $M = 1299.4$, orthorhombic, space group $P2_12_12_1$ (no. 19), $a = 12.406(16)$, $b = 16.065(9)$, $c = 21.851(8)$ Å, $U = 4355\ (9)$ $Å^3$, $T = 298$ K, $Z = 4$, μ(Mo-Kα) = 1.7 mm^{-1}, $D_c = 1.982$ g cm^{-3}.

The intensity data were collected at room temperature on a CAD4 Enraf-Nonius diffractometer, using graphite-monochromated Mo-Kα radiation. Two reference reflections were periodically monitored for intensity and orientation control. An overall decay of 27% was observed, despite the use of a crystal coated with oil in a Lindeman tube. A total of 4272 reflections were measured ($2 < 2\theta < 50°$) using the 2θ–ω method. Intensities were corrected for Lorentz-polarization effects and a absorption correction was carried out using DIFABS.[26] The structure was solved by direct methods,[27] neutral-atom scattering factors were used, and anomalous dispersion corrections were included.[28] Hydrogen atoms were not included in the model. Distances and angles within the tetrabutylammonium cation were constrained to 1.55 ± 0.05 Å and 109 ± 1°, respectively. All atoms were given anisotropic thermal parameters. Refinements were carried out by full matrix least-square procedures. The refinement of the 497 parameters converged at $R1 = 0.054$ and $wR(F^2) = 0.060$ ($w = 1$) for 2794 reflections [$I > 3\sigma(I)$]. Largest peak and hole in the final difference map were +1.36, −1.65 e $Å^{-3}$. All computations were performed using the CRYSTALS version for PC.[29] Selected bond lengths and angles are listed in Table 1. A CAMERON view[30] of the anion is depicted on Fig. 1.

CCDC reference number 186/1232.

See http://www.rsc.org/suppdata/dt/1999/51/ for crystallographic files in .cif format.

Results and discussion

Syntheses

The synthesis and the X-ray characterization of $[C_5Me_5O][Mo_6Cp^*O_{18}]$ were reported by Bottomley and Chen[17] in 1992. This compound formed from a mixture of $[(MoCp^*O_2)_2(\mu\text{-}O)]$ and $[MoCp^*ClO_2]$ resulting from air oxidation of $[\{MoCp^*(CO)_2\}_2]$ in $CHCl_3$. Harper and Rheingold[31] had previously described the sealed-tube preparation of $[W_6Cp^*_2O_{17}]$ by reaction of $[\{WCp^*(CO)_2\}_2]$ with methylarsaoxanes $(MeAsO)_n$. Both $[Mo_6Cp^*O_{18}]^-$ and $[W_6Cp^*_2O_{17}]$ molecular structures derive from that of the Lindqvist-type polyoxoanion $[M_6O_{19}]^{2-}$ [32] by formal replacement of one or two oxo ligands by Cp* ligand(s) (see below). As we are currently involved in a systematic study of functionalized polyoxoanions,[18–23] we decided to explore the condensation reactions of the $[MCp^*O_3]^-$ (M = Mo or W) anions,[25] both to improve the syntheses of $[Mo_6Cp^*O_{18}]^-$ and $[W_6Cp^*_2O_{17}]$ and eventually to characterize novel cyclopentadienyl–oxo polyanions. Indeed it was anticipated that acid-driven condensation of $[MCp^*O_3]^-$ could afford Cp*–oxo polyanions, just as that of the parent $[MO_4]^{2-}$ anions results in the formation of polyoxoanions. In parallel to acidification reactions, which are under investigation, we looked at the self-assembly reactions of polyoxometalate precursors and $[MoCp^*O_3]^-$. Up to now, the only characterized product of the reaction between $[MoCp^*O_3]^-$ anion and $[MoO_2(acac)_2]$, as a potential source of MoO_2^{2+}, is $[Mo_6O_{19}]^{2-}$. On the other hand, $[n\text{-}Bu_4N]_2[Mo_4O_{10}(OMe)_4Cl_2]$, which is known to transform into $[n\text{-}Bu_4N]_2[Mo_6O_{19}]$ in refluxing methanol, reacts with an equivalent of $[n\text{-}Bu_4N][MoCp^*O_3]$ in methanol to afford red-orange crystals of $[n\text{-}Bu_4N][Mo_6Cp^*O_{18}]$ in reasonable yield. The synthesis of $[n\text{-}Bu_4N]_2[Mo_4O_{10}(OMe)_4Cl_2]$ was first described by Zubieta and coworkers,[33] and was subsequently improved in our group by treating $Me_2NOH\cdot HCl$ with $[n\text{-}Bu_4N]_4[\alpha\text{-}Mo_8O_{26}]$ in methanol. Although the exact role of the dimethylhydroxylamine is not clear, similar attempts with hydrochloric acid in place of $Me_2NOH\cdot HCl$ have failed up to now. The $[Mo_4O_{10}(OMe)_4Cl_2]^{2-}$ anion consists of a compact arrangement of edge-sharing octahedra, with two doubly and two triply bridging methoxo ligands. The chloro ligands occupy terminal sites.

The IR spectrum of $[n\text{-}Bu_4N][Mo_6Cp^*O_{18}]$ in the 1000–250 cm^{-1} range is typical of a Lindqvist-type species and is in accordance with that previously reported by Bottomley and Chen[17] for $[C_5Me_5O][Mo_6Cp^*O_{18}]$. The IR spectrum of $[n\text{-}Bu_4N]_2[Mo_6O_{19}]$ displays two main bands at 954 and 800 cm^{-1}, attributed to the ν_{asym}(Mo=O_t) (F_{1u}) and ν_{asym}(Mo–O–Mo) vibrational modes respectively.[34] A splitting of these two characteristic bands is actually observed in the spectrum of $[n\text{-}Bu_4N][Mo_6Cp^*O_{18}]$ which shows peaks at 982, 955, 798 and 778 cm^{-1}. This is typical of monofunctionalized Lindqvist-type hexamolybdates and reflects the anion symmetry lowering from O_h to C_{4v} on substitution.[21,22,35,36]

The electronic spectrum of $[n\text{-}Bu_4N][Mo_6Cp^*O_{18}]$ was recorded in acetonitrile solution. A broad ligand-to-metal charge-transfer absorption is observed at 258 nm (log $\varepsilon = 4.5$) with two shoulders at 283 (log $\varepsilon = 4.4$) and 494 nm (log $\varepsilon = 2.35$). By comparison, the spectrum of $[n\text{-}Bu_4N]_2[Mo_6O_{19}]$ displays a peak at 260 (log $\varepsilon = 4.2$) and a shoulder at 325 nm (log $\varepsilon = 4.0$). These features account for the change from yellow $[n\text{-}Bu_4N]_2[Mo_6O_{19}]$ to orange-red $[n\text{-}Bu_4N][Mo_6Cp^*O_{18}]$. If the

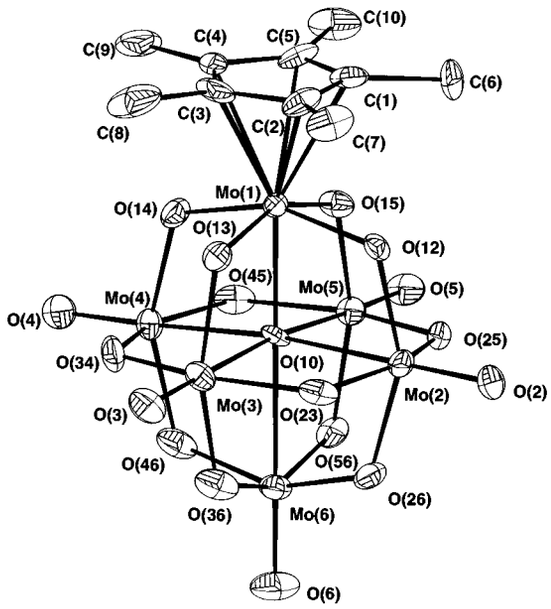

Fig. 1 Molecular structure of the anion $[Mo_6Cp^*O_{18}]^-$.

absorption at 494 nm is assumed to involve charge transfer from the Cp* ligand, then this supports the conclusion that the latter is a stronger donor than the oxo ligand (see below). This is in keeping with prevailing views that the Cp ligand is a stronger donor than the *t*-BuN ligand,[37] which is itself a stronger donor than the oxo ligand.[38]

Structure analysis

The molecular structure of the anion of $[n\text{-}Bu_4N][Mo_6Cp^*O_{18}]\cdot Me_2CO$ (Fig. 1) is closely related to that of $[Mo_6O_{19}]^{2-}$ [39] by formal replacement of a terminal oxo ligand by a η^5-Cp* ligand, both ligands being able to form $\sigma,2\pi$ triple bonds.

The distance of Mo(1) to the mean plane through the Cp* ligand is 2.083 Å, while the average of the Mo(1)–C(*i*) (*i* = 1–5) distances is 2.40 Å. Previous structural studies of substituted Lindqvist-type hexamolybdates including the $C_5Me_5O^+$ salt of $[Mo_6Cp^*O_{18}]^-$ reported by Bottomley and Chen,[17] $[CpTiMo_5O_{18}]^{3-}$,[35] the imido $[Mo_6O_{18}(NC_6H_4Me\text{-}p)]^{2-}$,[36] diazenido $[Mo_6O_{18}(NNC_6F_5)]^{3-}$,[40] and hydrazido $[Mo_6O_{18}(NNMePh)]^{2-}$ [41] derivatives have emphasized the geometrical distortions related to the substitution. Owing to the relatively low precision of the structural data for $[n\text{-}Bu_4N][Mo_6Cp^*O_{18}]\cdot Me_2CO$, the alteration, in those of the $M_4(\mu\text{-}O)_4$ rings involving the substituted centre, of the regular *trans*-alternation pattern of long and short bond lengths observed for $[Mo_6O_{19}]^{2-}$ is unclear. However, the balance of Mo(*i*)–O(10) distances indicates a significant displacement of the central oxygen atom O(10) towards Mo(1) [Mo(1)–O(10) 2.14 (1), Mo(6)–O(10) 2.48 (1), average Mo_{eq}–O(10) 2.33 Å]. This is in close agreement with the reported data for $[C_5Me_5O][Mo_6Cp^*O_{18}]$.[17] This is the largest deviation observed in a Lindqvist derivative and reflects the weak *trans* influence of the η^5-Cp* ligand. Indeed, structural data for complexes of the type $[ReCp^*XCl_2]$ (X = O [42] or *t*-BuN [43]) clearly show that the *trans* influence decreases along the series O > NR ⩾ Cp*.

Electrochemical studies

As expected, the $[Mo_6Cp^*O_{18}]^-$ anion is electrochemically active. The voltammogram of $[n\text{-}Bu_4N][Mo_6Cp^*O_{18}]$ in acetonitrile at a carbon electrode displays a reversible ($E_{p_a} - E_{p_c}$ = 0.068 V) reduction process at −0.033 V *vs*. SCE, as depicted in Fig. 2. No further reduction process could be clearly observed, due to adsorption effects. On the other hand, the polarogram of $[n\text{-}Bu_4N][Mo_6Cp^*O_{18}]$ in acetonitrile at a dropping mercury electrode displays three well defined waves, at −0.09, −1.04 and −1.44 V *vs*. SCE respectively, each of which involves one electron by comparison with $[n\text{-}Bu_4N]_2[Mo_6O_{19}]$. The positive shift of the first reduction process of $[Mo_6Cp^*O_{18}]^-$, compared to $[Mo_6O_{19}]^{2-}$ ($E = -0.37$ V), reflects the effect of the overall charge lowering on substitution. It should be even larger if it were not for the strong donation from the Cp* ligand.

Table 1 Selected distances (Å) and bond angles (°) for $[n\text{-}Bu_4N][Mo_6Cp^*O_{18}]\cdot Me_2CO$

Mo(1)–O(10)	2.14(1)	Mo(1)–O(12)	1.94(2)
Mo(1)–O(13)	1.91(2)	Mo(1)–O(14)	1.88(2)
Mo(1)–O(15)	1.87(2)	Mo(1)–C(1)	2.38(3)
Mo(1)–C(2)	2.34(2)	Mo(1)–C(3)	2.40(3)
Mo(1)–C(4)	2.45(3)	Mo(1)–C(5)	2.44(3)
Mo(2)–O(2)	1.67(2)	Mo(2)–O(10)	2.33(1)
Mo(2)–O(12)	1.90(2)	Mo(2)–O(23)	1.92(2)
Mo(2)–O(25)	1.93(2)	Mo(2)–O(26)	1.97(2)
Mo(3)–O(3)	1.68(2)	Mo(3)–O(10)	2.33(1)
Mo(3)–O(13)	1.92(2)	Mo(3)–O(23)	1.96(2)
Mo(3)–O(34)	1.96(2)	Mo(3)–O(36)	1.97(2)
Mo(4)–O(4)	1.68(2)	Mo(4)–O(10)	2.33(1)
Mo(4)–O(14)	1.95(2)	Mo(4)–O(34)	1.90(2)
Mo(4)–O(45)	1.94(2)	Mo(4)–O(46)	1.95(2)
Mo(5)–O(5)	1.65(2)	Mo(5)–O(10)	2.34(2)
Mo(5)–O(15)	1.93(2)	Mo(5)–O(25)	1.95(2)
Mo(5)–O(45)	1.94(2)	Mo(5)–O(56)	1.94(2)
Mo(6)–O(6)	1.62(2)	Mo(6)–O(10)	2.48(1)
Mo(6)–O(26)	1.85(2)	Mo(6)–O(36)	1.84(2)
Mo(6)–O(46)	1.87(2)	Mo(6)–O(56)	1.86(2)
Mo(1)–O(12)–Mo(2)	116.2(7)	Mo(1)–O(13)–Mo(3)	116.5(8)
Mo(1)–O(14)–Mo(4)	115.9(8)	Mo(1)–O(15)–Mo(5)	116.8(8)
Mo(2)–O(23)–Mo(3)	115.2(6)	Mo(2)–O(25)–Mo(5)	116.4(7)
Mo(2)–O(26)–Mo(6)	119.8(9)	Mo(3)–O(34)–Mo(4)	117.4(8)
Mo(3)–O(36)–Mo(6)	120.4(10)	Mo(4)–O(45)–Mo(5)	115.8(6)
Mo(4)–O(46)–Mo(6)	119.6(9)	Mo(5)–O(56)–Mo(6)	120.7(8)

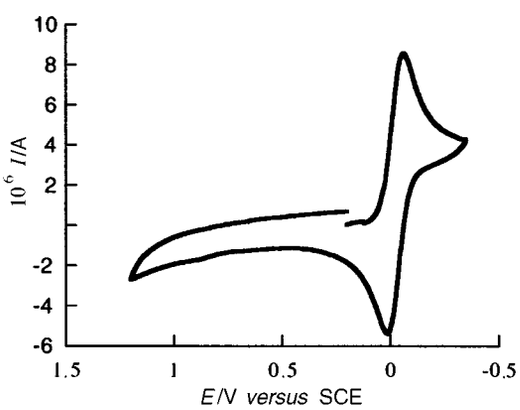

Fig. 2 Cyclic voltammogram of $[n\text{-}Bu_4N][Mo_6Cp^*O_{18}]$ in CH_3CN, at a carbon electrode *vs*. SCE at a scan rate of 0.1 V s^{-1}.

NMR studies

An exhaustive characterization of $[Mo_6Cp^*O_{18}]^-$ by multinuclear NMR has been performed. The ^{95}Mo and ^{17}O spectra are presented in Figs. 3 and 4 respectively.

On the basis of C_{4v} symmetry for the $[Mo_6Cp^*O_{18}]^-$ anion in solution, three signals are expected in the ^{95}Mo NMR spectrum. They are indeed observed at δ 175, 164 and −35, with respective intensities of 1 : 4 : 1. Let us observe that the signal from the four equivalent equatorial Mo atoms is quite narrow ($\Delta\nu_{\frac{1}{2}} \approx 60$ Hz) with respect to the two other ones ($\Delta\nu_{\frac{1}{2}} \approx 200$ Hz). This is consistent with a short quadrupolar relaxation rate (larger T_2) for the equatorial sites, according to a smaller electric field gradient for a less distorted site symmetry (see above).

Table 2 Selected NMR data for $[Mo_6O_{19}]^{2-}$ derivatives

Complex	$\delta(^{95}Mo)^a$	$\delta(^{17}O)^a$	
		O_t	μ-O
$[Mo_6O_{19}]^{2-}$ [41]	125 (6)	934 (6)	565 (12)
$[CpTiMo_5O_{18}]^{3-}$ [35]		863 (4), 834 (1)	641 (4), 535 (4), 516 (4)
$[VMo_5O_{19}]^{3-}$ [46]		1200 (1), 885 (5)	665 (4), 541 (4), 531 (4)
$[Mo_6O_{18}(NC_6H_4NO_2)]^{2-}$ [44]	143 (5), 51 (1)	923 (4), 914 (1)	581 (4), 567 (4), 555 (4)
$[Mo_6Cp^*O_{18}]^-$	175 (1), −35 (1) 164 (4)	931 (4), 890 (1)	613 (4), 580 (4), 559 (4)

[a] δ in ppm; multiplicity in parentheses.

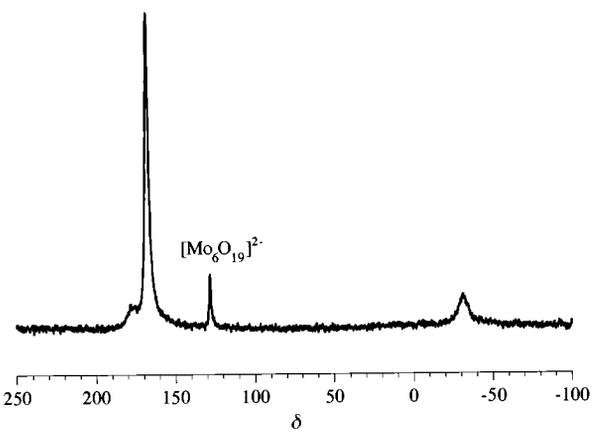

Fig. 3 The ^{95}Mo NMR spectrum of $[n\text{-}Bu_4N][Mo_6Cp^*O_{18}]$ in CH_3CN–CD_3CN, recorded at 343 K.

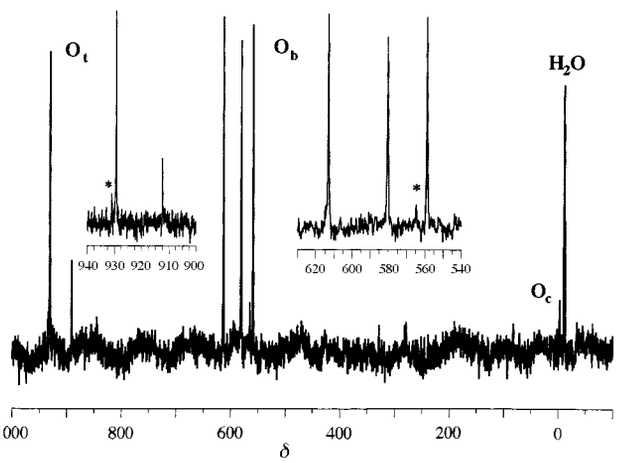

Fig. 4 Natural abundance ^{17}O NMR spectrum of $[n\text{-}Bu_4N][Mo_6Cp^*O_{18}]$ in CH_3CN–CD_3CN, recorded at 343 K. * Represents the $[Mo_6O_{19}]^{2-}$ impurity.

Our parallel studies of the imido series $[Mo_6O_{18}(NC_6H_4Z\text{-}p)]^{2-}$ (Z = OMe, Me, H, F, Cl, Br, CF_3 or NO_2) have shown that the expected signals for the Mo atoms bearing a terminal oxo ligand are lightly deshielded (less than 30 ppm) with respect to $[Mo_6O_{19}]^{2-}$ and that they are hardly resolved. On the contrary, the Mo bearing the imido ligand is significantly shielded, to an extent which depends on Z. The corresponding signal is indeed unambiguously assigned since it appears as a 1:1:1 triplet due to scalar $^1J(^{95}Mo–^{14}N)$ coupling.[22,44] Accordingly, the most shielded signal at δ −35 for $[Mo_6Cp^*O_{18}]^-$ should be attributed to the Mo atom bearing the Cp* ligand and the two other signals at δ 175 and 164 to the two other types of Mo.

If we assume a predominant diamagnetic contribution to the ^{95}Mo shielding, at least if the paramagnetic contribution is supposed to be nearly constant in these high-valent hexamolybdates, which seems reasonable since none of them has low-lying vacant electronic levels, then ^{95}Mo NMR data further suggest that donation decreases along the series Cp* > NR (R = aryl) > O, which also simply correlates with the softness of the attached ligand.†

The natural-abundance ^{17}O NMR spectrum of $[n\text{-}Bu_4N][Mo_6Cp^*O_{18}]$ has been measured in CH_3CN–CD_3CN at 343 K in order to reduce the signal linewidth. It displays a pattern of six lines at δ 931, 890, 613, 580, 559 and −2.7. As ^{17}O chemical shifts of polyoxometalates correlate with the metal–oxygen π-bond order,[45] assignment of the resonances is straightforward: the two most deshielded lines (4:1) are assigned to the two types of terminal oxo ligands (O_t), the three close lines (4:4:4) around δ 600 to the three types of symmetry non-equivalent μ-O ligand (O_b) and finally the most shielded one at δ −2.7 to the central oxygen atom (O_c). Owing to the large distortion of the Mo_6O_c octahedron with respect to O_h symmetry, O_c should experience a relatively large electric field gradient, which favours the quadrupolar relaxation of this nucleus; this explains why the O_c resonance could be observed for $[Mo_6Cp^*O_{18}]^-$, whereas this line was hardly (or not) detected for nitrosyl derivatives under the same experimental conditions of quick pulse repetition (20 Hz).[21]

When considering the weighted average chemical shift for each set of oxygen atoms, it appears that μ-O are deshielded, while terminal oxygen atoms are shielded, with respect to the parent anion $[Mo_6O_{19}]^{2-}$ (Table 2). The decrease of the overall charge from $[Mo_6O_{19}]^{2-}$ to $[Mo_6Cp^*O_{18}]^-$ should lead to a deshielding of all oxygen resonances. Therefore the net shielding of the terminal oxygen atoms suggests that some other effect of the Cp* ligand prevails over the charge effect. This further supports the conclusion that Cp* is a better donor than the oxo ligand. Moreover the weighted average $\delta(O_t)$ is nearly the same for the $[Mo_6Cp^*O_{18}]^-$ monoanion (923) and for the $[Mo_6O_{18}(NC_6H_4NO_2\text{-}p)]^{2-}$ dianion (921), which suggests that the Cp* ligand is a better donor than the imido ligands, in agreement with the conclusions from ^{95}Mo NMR data.

Concluding remarks

The Lindqvist-type derivative $[n\text{-}Bu_4N][Mo_6Cp^*O_{18}]$ has been successfully prepared by reaction of $[n\text{-}Bu_4N][MoCp^*O_3]$ with $[n\text{-}Bu_4N]_2[Mo_4O_{10}(OMe)_4Cl_2]$ in methanol, and has been characterized by single-crystal X-ray diffraction and multinuclear NMR in solution. We are currently exploiting the potential of $[MoCp^*O_3]^-$ and of its tungsten analogue in the syntheses of Cp*–oxo polyanions by triggering the condensation with different Brönsted and Lewis acids.

References

1 P. Gouzerh and A. Proust, *Chem. Rev.*, 1998, **98**, 77.
2 K. Isobe, *Acc. Chem. Res.*, 1993, **26**, 524.
3 Y. Hayashi, Y. Ozawa and K. Isobe, *Chem. Lett.*, 1989, 425.
4 H. K. Chae, W. G. Klemperer and V. W. Day, *Inorg. Chem.*, 1989, **28**, 1423.
5 V. W. Day and W. G. Klemperer, *Polyoxometalates: from Platonic*

† The correlation of the metal chemical shift with the softness of the ligand has been suggested by a referee.

Solids to Anti-retroviral Activity, eds. M. T. Pope and A. Müller, Kluwer, Dordrecht, 1994, p. 87.
6 R. G. Finke and M. W. Droege, *J. Am. Chem. Soc.*, 1984, **106**, 7274.
7 R. G. Finke, B. Rapko and P. J. Domaille, *Organometallics*, 1986, **5**, 175.
8 D. J. Edlung, R. J. Saxton, D. K. Lyon and R. G. Finke, *Organometallics*, 1988, **7**, 1692.
9 Y. Lin, K. Nomiya and R. G. Finke, *Inorg. Chem.*, 1993, **32**, 6040.
10 M. Pohl and R. G. Finke, *Organometallics*, 1993, **12**, 1453.
11 B. Rapko, M. Pohl and R. G. Finke, *Inorg. Chem.*, 1994, **33**, 3625.
12 T. Nagata, M. Pohl, H. Weiner and R. G. Finke, *Inorg. Chem.*, 1997, **36**, 1366.
13 N. Mizuno, H. Weiner and R. G. Finke, *J. Mol. Catal.*, 1996, **114**, 15.
14 J. D. Aiken III, Y. Lin and R. G. Finke, *J. Mol. Catal.*, 1996, **114**, 29.
15 A. R. Siedle, C. G. Markell, P. A. Lyon, K. O. Hodgson and A. L. Roe, *Inorg. Chem.*, 1987, **26**, 219.
16 F. Bottomley and L. Sutin, *Adv. Organomet. Chem.*, 1988, **28**, 339.
17 F. Bottomley and J. Chen, *Organometallics*, 1992, **11**, 3404.
18 P. Gouzerh, Y. Jeannin, A. Proust and F. Robert, *Angew. Chem.*, *Int. Ed. Engl.*, 1989, **28**, 1363.
19 A. Proust, P. Gouzerh and F. Robert, *Inorg. Chem.*, 1993, **32**, 5291.
20 A. Proust, R. Thouvenot, F. Robert and P. Gouzerh, *Inorg. Chem.*, 1993, **32**, 5299.
21 A. Proust, R. Thouvenot, S.-G. Roh, J.-K. Yoo and P. Gouzerh, *Inorg. Chem.*, 1995, **34**, 4106.
22 A. Proust, R. Thouvenot, M. Chaussade, F. Robert and P. Gouzerh, *Inorg. Chim. Acta*, 1994, **224**, 81.
23 A. Proust, S. Taunier, V. Artero, F. Robert, R. Thouvenot and P. Gouzerh, *Chem. Commun.*, 1996, 2195.
24 N. H. Hur, W. G. Klemperer and R.-C. Wang, *Inorg. Synth.*, 1990, **27**, 78.
25 M. S. Rau, C. M. Kretz, L. A. Mercando, G. L. Geoffroy and A. L. Rheingold, *Organometallics*, 1993, **12**, 3447.
26 N. Walker and D. Stuart, *Acta Crystallogr.*, *Sect. A*, 1983, **39**, 158.
27 G. M. Sheldrick, SHELXS 86, Program for Crystal Structure Determinations, University of Göttingen, 1986.
28 *International Tables for X-Ray Crystallography*, Kynoch Press, Birmingham, 1974, vol. IV, p. 149.
29 D. J. Watkin, C. K. Prout, J. R. Carruthers and P. W. Betteridge, CRYSTALS, Chemical Crystallography Laboratory, University of Oxford, Oxford, 1996.
30 D. J. Watkin, C. K. Prout and L. J. Pearce, CAMERON, Chemical Crystallography Laboratory, University of Oxford, 1996.
31 J. R. Harper and A. L. Rheingold, *J. Am. Chem. Soc.*, 1990, **112**, 4037.
32 M. T. Pope, *Heteropoly and Isopoly Oxometalates*, Springer, Berlin, 1983.
33 H. Kang, S. Liu, S.-N. Shaikh, T. Nicholson and J. Zubieta, *Inorg. Chem.*, 1989, **28**, 920.
34 C. Rocchiccioli-Deltcheff, R. Thouvenot and M. Fouassier, *Inorg. Chem.*, 1982, **21**, 30.
35 T. M. Che, V. W. Day, L. C. Francesconi, M. F. Fredrich, W. G. Klemperer and W. Shum, *Inorg. Chem.*, 1985, **24**, 4055.
36 Y. H. Du, A. L. Rheingold and E. A. Maatta, *J. Am. Chem. Soc.*, 1992, **114**, 345.
37 J. Sundermeyer and D. Runge, *Angew. Chem.*, *Int. Ed. Engl.*, 1994, **33**, 1255.
38 W. A. Nugent and J. M. Mayer, *Metal–Ligand Multiple Bonds*, Wiley, New York, 1988.
39 H. R. Allcock, E. C. Bissel and E. T. Shawl, *Inorg. Chem.*, 1973, **12**, 2963.
40 S. Bank, S. Liu, S.-N. Shaikh, X. Sun, J. Zubieta and P. D. Ellis, *Inorg. Chem.*, 1988, **27**, 3535.
41 H. Kang and J. Zubieta, *J. Chem. Soc.*, *Chem. Commun.*, 1988, 1192.
42 W. A. Herrmann, E. Herdtweck, M. Flöel, J. Kulpe, U. Küsthardt and J. Okuda, *Polyhedron*, 1987, **6**, 155.
43 W. A. Herrmann, G. Weichselbaumer, R. A. Paciello, R. A. Fischer, D. Herdtweck, J. Okuda and D. W. Marz, *Organometallics*, 1990, **9**, 489.
44 S. Taunier, A. Proust, R. Thouvenot and P. Gouzerh, unpublished work.
45 W. G. Klemperer, *Angew. Chem.*, *Int. Ed. Engl.*, 1978, **17**, 246.
46 M. Filowitz, R. K. C. Ho, W. G. Klemperer and W. Shum, *Inorg. Chem.*, 1979, **18**, 93.

Paper 8/05832F